CO_2 Adsorption

International Edition: DOI: 10.1002/anie.201812363
German Edition: DOI: 10.1002/ange.201812363

Prediction of Carbon Dioxide Adsorption via Deep Learning

Zihao Zhang, Jennifer A. Schott, Miaomiao Liu, Hao Chen, Xiuyang Lu, Bobby G. Sumpter, Jie Fu, and Sheng Dai**

Abstract: *Porous carbons with different textural properties exhibit great differences in CO_2 adsorption capacity. It is generally known that narrow micropores contribute to higher CO_2 adsorption capacity. However, it is still unclear what role each variable in the textural properties plays in CO_2 adsorption. Herein, a deep neural network is trained as a generative model to direct the relationship between CO_2 adsorption of porous carbons and corresponding textural properties. The trained neural network is further employed as an implicit model to estimate its ability to predict the CO_2 adsorption capacity of unknown porous carbons. Interestingly, the practical CO_2 adsorption amounts are in good agreement with predicted values using surface area, micropore and mesopore volumes as the input values simultaneously. This unprecedented deep learning neural network (DNN) approach, a type of machine learning algorithm, exhibits great potential to predict gas adsorption and guide the development of next-generation carbons.*

The CO_2 concentration in the atmosphere has gone up rapidly in recent years, which causes great concern regarding the environment.[1] Many efforts have been devoted to efficient CO_2 capture and storage, the main technologies for which are cryogenic and membrane separation, as well as chemical and physical adsorption.[2] Among these, adsorption technologies are now considered the most promising method because of their controllability, simplicity, low cost, low energy demand, high adsorption capacity, and other qualities.[3] Recently, the development of porous materials for CO_2 adsorption, such as zeolites,[4a,b] mesoporous silica,[4c] microporous organic polymers,[4d] metal–organic frameworks (MOFs),[4e] covalent-organic frameworks (COFs)[4f] and porous carbons[4g,h]—has attracted much attention. To date, carbon-based materials are one of the most promising adsorbents for CO_2 capture because of their low cost, fast adsorption-desorption kinetics, large surface area and pore volume, as well as easy-to-design pore structure.[2a,5]

Porous carbon materials can be synthesized using various methods, and the obtained surface parameters such as surface area (S_{BET}), mesopore volume (V_{meso}), micropore volume (V_{micro}), and so on vary greatly.[5a,6] To improve CO_2 uptake, much research effort has been dedicated to designing a porous carbon material with high S_{BET} and pore volume.[1b,2b,6a,7] The KOH activation and template-assisted methods are considered as the most efficient approaches.[8] For example, He et al. used zeolite as a template to enhance the surface area and pore volume of microporous carbon-based materials to obtain high CO_2 adsorption.[9] Nowadays, it is widely accepted that narrow micropores are the major factor in CO_2 adsorption;[5c] however, the detailed relationship between pore structure and CO_2 adsorption remains unclear. This deficiency in structure–property relationships hampers the development of next-generation carbon adsorbents and advanced gas adsorbents in general.

There are many phenomenological attempts to fill this knowledge gap. Notably, the interesting recent work by Clark, North, and co-workers have shown the CO_2 adsorption capacity is surprisingly affected by V_{meso} through the nonlinear product term of V_{micro} and V_{meso} shown in Equation (1):[3a] They showed the CO_2 physisorption to be the predominant adsorption mechanism.[3a] A partial least squares regression approach was used to predict CO_2 adsorption, as shown in Equation (1).[3a] Although this regression equation is capable of making a reasonable fitting, it is difficult to obtain an ideal empirical formula according to the regression polynomials method. Moreover, this equation lacks the ability to learn and improve as the database grows.[10] More important, ordered mesoporous carbon without micropores should have almost no ability to adsorb CO_2 according to Equation (1), which is unreasonable in some cases.

$$M_{ads}^{CO_2} = 0.095 + 2.10\,V_{micro} + 3.51\,V_{micro}\,V_{meso} \quad (1)$$

Machine learning using algorithms allows computers to identify the relationship among different variables to provide underlying instructions even for nonlinear interpolations.[11] Artificial neural networks (NNs) as a type of machine learning algorithm, can achieve optimized results by adjusting the synapse weights.[12] Neurons arranged in each layer need to be connected together into an NN.[12b] Among these, deep neural networks (DNNs) with more than one hidden layer

[*] Z. Zhang, Dr. H. Chen, Dr. X. Lu, Dr. J. Fu
Key Laboratory of Biomass Chemical Engineering of Ministry of Education, College of Chemical and Biological Engineering
Zhejiang University
Hangzhou 310027 (China)
E-mail: jiefu@zju.edu.cn
Z. Zhang, J. A. Schott, Dr. S. Dai
Chemical Sciences Division, Oak Ridge National Laboratory
Oak Ridge, TN (USA)
Z. Zhang, J. A. Schott, M. Liu, Dr. S. Dai
Department of Chemistry
University of Tennessee
Knoxville, TN (USA)
E-mail: dais@ornl.gov
Dr. B. G. Sumpter
Center for Nanophase Materials Sciences, Oak Ridge National Laboratory
Oak Ridge, TN (USA)
Supporting information and the ORCID identification number(s) for the author(s) of this article can be found under: https://doi.org/10.1002/anie.201812363.

have been shown to surpass state-of-the-art models in a diversity of applications.[13] Although the application of deep learning to chemistry-relevant problems remains in its infancy, the situation has been changing quickly.[13,14] To date, little research has been able to make suitable predictions for CO_2 adsorption using known textural parameters of porous carbons.[7]

Herein, we describe three NNs trained with 12 known data points reported from Clark, North, and co-workers shown in Table S1 in the Supporting Information using V_{micro}, V_{micro}-V_{meso} and V_{micro}-V_{meso}-S_{BET} as the input neurons, respectively.[3] Then, the NNs with an implicit relationship between the textural properties and CO_2 adsorption is employed to predict the possible CO_2 adsorption capacities of six porous carbons synthesized in our lab. To make the predictions more widely useful, we screen more than 1000 CO_2 adsorption data of porous carbons at different adsorption conditions and train a DNN with two hidden layers using the adsorption conditions (temperature and pressure) and textural properties as variables. The deep learning method was capable of automatically predicting the CO_2 adsorption capacity of 20 randomly untrained porous carbons regardless of their synthesis method, raw materials, or specific structure. This unprecedented DNN approach exhibits great potential to predict the gas adsorption capacities of porous materials using their textural properties, as shown in Scheme 1.

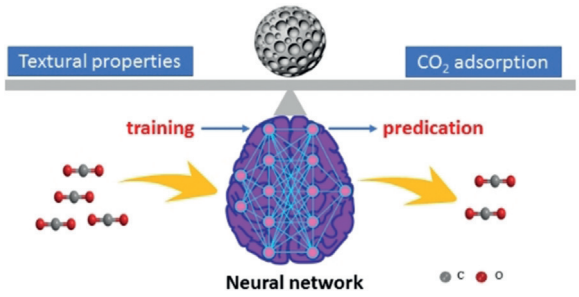

Scheme 1. The prediction of CO_2 adsorption of porous carbon.

The Brunauer-Emmett-Teller surface area (S_{BET}), V_{micro}, and V_{meso} of different porous carbon materials synthesized in our lab are summarized in Table 1. MC-450, MC-600, and MC-850 synthesized using an enhanced hydrogen-bonding interaction method[15] (mesoporous carbons with pyrolysis temperatures of 450, 600, and 850 °C, respectively) were chosen as the predicted samples. All as-synthesized mesoporous carbons had total pore volumes of over 0.5 $cm^3 g^{-1}$ with a very low micropore volume, indicating they were predominantly mesoporous materials. The N_2 adsorption–desorption isotherms in Figure 1a also exhibit a type IV isotherm with remarkable hysteresis loops at $P/P_0 = 0.6$–0.8, suggesting the existence of uniform mesoporosity. Additionally, the S_{BET} and V_{total} of the mesoporous carbons increased as the pyrolysis temperature increased in Table 1.

Table 1: The textural properties of different porous carbons.

Samples	S_{BET} [$m^2 g^{-1}$]	V_{total} [$cm^3 g^{-1}$]	V_{micro} [$cm^3 g^{-1}$]	V_{meso} [$cm^3 g^{-1}$]
MC-450	346	0.51	0.05	0.46
MC-600	390	0.60	0.05	0.55
MC-850	451	0.67	0.06	0.61
AC Darco	625	0.57	0.14	0.43
AC Charcoal	1327	0.61	0.35	0.26
Vulcan XC605	55	0.16	0	0.16

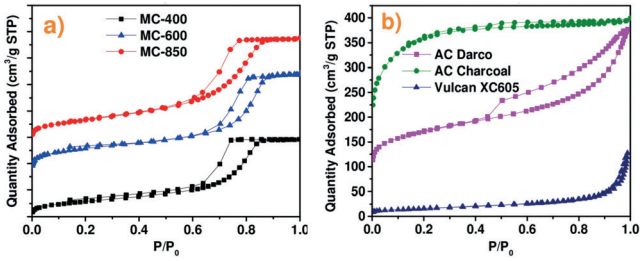

Figure 1. N_2 adsorption–desorption isotherms at 77 K of predicted porous carbons.

To make the predication scope more extensive, a commercial activated carbon, Darco (AC Darco), activated cocoanut charcoal (AC charcoal), and Vulcan XC605 were selected as another three predicted samples. The S_{BET} of AC Darco in Table 1 was 625 $m^2 g^{-1}$ with V_{micro} of 0.14 $cm^3 g^{-1}$ and V_{meso} of 0.43 $cm^3 g^{-1}$. The N_2 adsorption-desorption isotherms of AC Darco exhibited a plateau starting at a very low relative pressure and typical IV isotherm with a remarkable hysteresis loop, indicating a hierarchical porous structure. In comparison, AC charcoal showed a typical I isotherm with a highest surface area of 1327 $m^2 g^{-1}$ in Table 1 and Figure 1, suggesting it was predominantly microporous. Vulcan XC605 as a mesoporous material exhibited the lowest surface area, 55 $m^2 g^{-1}$, with almost no micropore volume.

To clarify the role of S_{BET}, V_{micro}, and V_{meso}, different variables were chosen as neurons, imported to the input layer, and passed in an orderly manner into the hidden layers and output layer. The information obtained from the NN was finally stored and transferred via a feed-forward process to predict the CO_2 adsorption of six porous carbon materials in our lab. Figure 2 exhibits a typical architecture of an NN; an NN with more than one hidden layer was considered a DNN. Each line between two nodes represents a weight, and the input-output relation can be simulated by changing these weights. To determine each weight, the NN was trained as countless by comparing the experimental and calculated output values and then adjusting the weights for every node to decrease the error.

The 12 porous carbon data points in Table S1 reported from Clark, North, and co-workers were chosen as the training objectives to obtain a correlation between CO_2 adsorption and textural properties.[3a] The CO_2 adsorption properties of six predicted samples in Table 1 were measured at the same experimental conditions with 12 training objectives. The average data obtained from four cycles are shown in Figure 3a. The experimental values of MC-400, MC-600, MC-

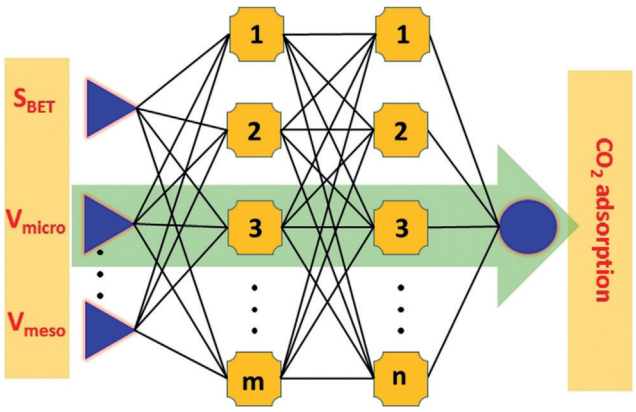

Figure 2. The typical architecture of an artificial neural network.

850, AC Darco, AC charcoal, and Vulcan XC605 were 1.36, 2.02, 2.25, 2.79, 5.46, and 0.32 mmol g^{-1}, respectively. The first NN (NN-1)-consisting of one hidden layer, one input (V_{micro}), and one output (CO_2 adsorption)-was established. Figure 3b exhibits the corresponding correlation plot for the 12 training objectives. The experimental and predicted data of 12 training objectives (12 black dots) were fitted, and the obtained NN-1 was further used to predict the CO_2 adsorption of the six tested samples using V_{micro} as the input value.

However, the experimental and predicted data from NN-1 showed significant discrepancy (six blue dots in Figure 3b), especially for the Vulcan XC605, AC Darco and AC charcoal samples. As a result, the obtained NN-1 could not be used as an ideal model for predicting the CO_2 adsorption capacities of porous carbon materials. These results indicated that V_{micro} in porous carbons is not the only determinant of CO_2 adsorption. Thereafter, the input layer with two neurons (V_{micro}, V_{meso}) was used to establish the second NN (NN-2). The optimized results in Figure 3c suggest that NN-2 exhibited better prediction behavior than NN-1, indicating mesopores also played an important role in CO_2 adsorption. However, the predicted CO_2 adsorption value of AC charcoal was 2.38 mmol g^{-1}, much lower than the experimental value of 5.46 mmol g^{-1}.

To clarify the reason, we carefully compared the textural properties and CO_2 adsorption data of AC charcoal with 12 training samples. We found that AC charcoal (0.61 $cm^3 g^{-1}$) had a similar V_{total} to that of commercial AC Norit (0.60 $cm^3 g^{-1}$) in Table S1.[3] The micropore and mesopore volumes of commercial Norit activated carbon are 0.42 and 0.18 $cm^3 g^{-1}$, respectively. The V_{total} of AC charcoal was slightly less, and its V_{micro} was very similar to that of AC Norit. As a result, the CO_2 adsorption values for AC charcoal and AC Norit obtained from Equation (1) should be similar. However, the practical CO_2 adsorption of AC charcoal, 5.46 mmol g^{-1}, was much higher than the 2.0 mmol g^{-1} of AC Norit. The predicted result for AC charcoal from NN-2 was 2.38 mmol g^{-1}, which was also lower than the practical data, but similar to the experimental data for AC Norit. Although the pore volumes were similar, the S_{BET} of AC charcoal was 1327 $m^2 g^{-1}$, much higher than the 798 $m^2 g^{-1}$ for AC Norit. It suggested the additional CO_2 adsorption capacity of AC charcoal compared with AC Norit might be related to its higher surface area.

Next, a NN with three neurons (S_{BET}, V_{micro}, and V_{meso}) was used to train 12 objectives. To confirm that the designed NN model was suitable for predicting the CO_2 adsorption capacity of porous carbon, the experimental and predicted results using this NN-3 were compared. The results are shown in Figure 3d. It was found that the results for the 12 training samples obtained from NN-3 were consistent with the experimental results (black dots). Thereafter, the S_{BET}, V_{micro}, and V_{meso} of six tested samples were chosen as the input values to check the predictive ability of NN-3. Surprisingly, the predicted results for the six tested samples obtained from BPNN-3 were very close to the experimental results (blue dots in Figure 3d).

It is undeniable that Equation (1) for the first time provided a detailed correlation between CO_2 adsorption and textural properties. However, the scope of application was very narrow (just for carbonaceous materials). For example, ordered mesoporous carbon with almost no micropores should have little ability to adsorb CO_2, according to Equation (1). However, mesoporous carbon with high CO_2 adsorption is seen in Figure 3a, suggesting Equation (1) is not applicable to these kinds of porous carbon materials. Moreover, we used this equation to predict values for the porous carbon materials in our lab and discovered the predicted and experimental results showed a big discrepancy.

To avoid the contingency of using a small amount of data, we collected more than 1000 CO_2 adsorption data for different porous carbons in Table S2. All

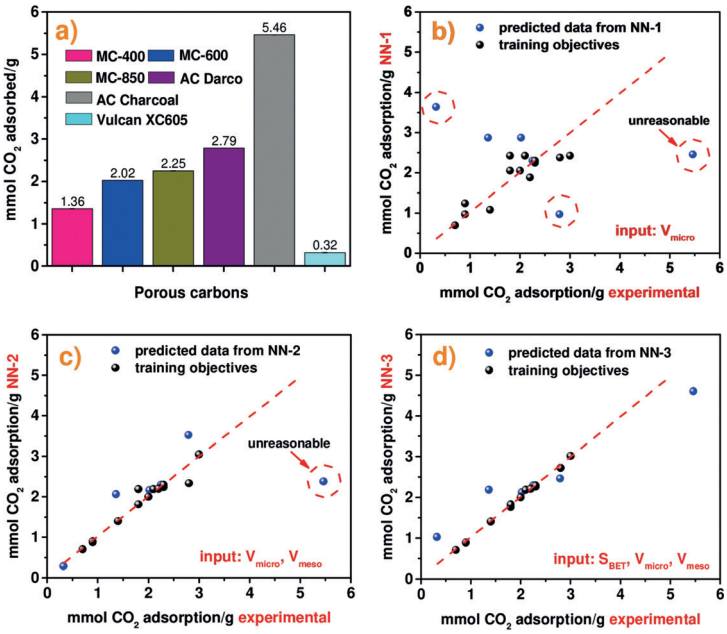

Figure 3. a) CO_2 adsorption data for different porous carbon samples. All data are the average of four measurements, and the error bars are very small. The correlations between CO_2 adsorption data achieved from experiment and estimated from the b) NN-1 (V_{micro}), c) NN-2 (V_{micro} and V_{meso}), and d) NN-3 (S_{BET}, V_{micro} and V_{meso}). See text for details.

porous carbons were screened without heteroatom N, since N has been confirmed to have a great influence on the CO_2 adsorption capacity. The surface area, micropore volume, and mesopore volume, as well as the adsorption temperature and pressure, were considered as five neurons in the input layer, as shown in Figure S1. Thereafter, we used a random 1000 samples as the training data to train a DNN with two hidden layers, and 20 date samples for cross-validation (prediction). Additionally, we use the leave-k-out method to check our model accuracy with the random 1000 training samples. This approach takes k examples from the total training data set of 1000 and uses those for predictions, then it repeats that $1000/k$ times so that you have an ensemble of test cases. Typically, it is most common to use $k = 1$, and then every single case is a test and the average error/performance gives a statistically significant indication of the accuracy of the neural network model. As shown in Figure 4a, remarkable agreement between experimental and predicted values was achieved for 1000 training samples. More importantly, the leave-one-out results reveal that the average error is only 0.43 for random 1000 training samples in Figure S2. Thus, a hidden correlation was discovered using a DNN to convert the input data (textural properties and adsorption conditions) to automatically discover new representations for output data (CO_2 adsorption). A very good prediction performance for the remaining 20 samples test case in Figure 4b indicates this DNN is suitable for the prediction of CO_2 adsorption. We believe that the error of the neural net model for the range of standard experimental results is totally acceptable.

Figure 4c describes the correlation between CO_2 adsorption and pore volume of porous carbons at the same adsorption conditions (25 °C and 1 bar) over more than 75 data points. We found that micropore and mesopore volume exhibited significantly different influences on CO_2 adsorption. The results demonstrated that the CO_2 uptake of porous carbons at ambient temperature and pressure conditions was mainly governed by the micropore volume, in good agreement with previous studies.[5] The mesopore volume also played an important role in CO_2 uptake. Although no clear role of mesopores can be summarized in Figure 4c, a small amount of mesoporosity did promote the ability of porous carbons to adsorb CO_2 in Figure S3. Moreover, excessive mesoporosity did little to promote CO_2 adsorption in some cases. In comparison, mesopores play a more important role on CO_2 adsorption under high pressure, as seen in Figure 4d. These results successfully explain a long-held reason why high CO_2 adsorption is always achieved under microporous carbons at low pressure, and obtained under hierarchical porous carbons at high pressure. Additionally, the correlation between CO_2 uptake, V_{micro} and S_{BET} was shown in Figure S4.

In this study, a remarkable agreement between experimental and predicted value about CO_2 adsorption capacity is achieved only when V_{micro}-V_{meso}-S_{BET} are chosen as the input neurons simultaneously. More importantly, the trained DNN can make an accurate prediction about CO_2 adsorption capacity for more than 1000 data samples collected from the literature and our lab. The key insights obtained are: First, our big data investigation further validated the importance of V_{meso} in controlling gas uptake, refuting a long-held notion that V_{micro} is an only parameter in controlling gas absorption of small molecules; Second, S_{BET} is an independent textural parameter that can be synergistically coupled with other textural parameters in determining gas–solid interactions and thus gas-uptake capacities; Third, the gas-uptake by solid adsorbents relies on the complex interplay among the textural parameters with the sensitivity of each parameter that can be estimated.

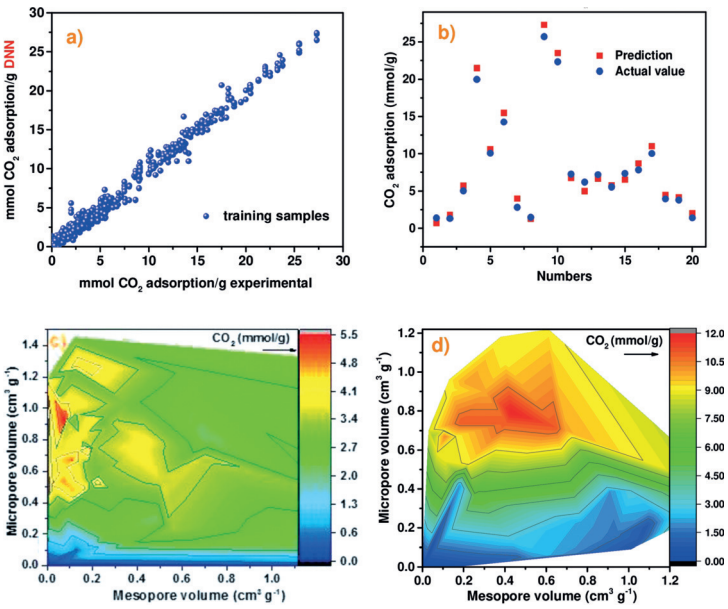

Figure 4. a) The correlation between CO_2 adsorption data achieved from experiment and estimated from DNN. b) The correlation between CO_2 adsorption data of 20 predicted sets achieved from experiment and estimated from trained DNN. c) The correlation between CO_2 uptake, micropore and mesopore volume at the same adsorption conditions (25 °C and 1 bar). d) The correlation between CO_2 uptake, micropore and mesopore volume at the same adsorption conditions (25 °C and 5 bar).

Acknowledgements

This work was supported by the Division of Chemical Sciences, Geosciences, and Biosciences, Office of Basic Energy Sciences, US Department of Energy. J.F. was supported by the National Natural Science Foundation of China (No. 21436007, 21676243, 21706228), the Zhejiang Provincial Natural Science Foundation of China (No. LR17B060002). Z.Z. thanks the China Scholarship Council for financial support as a joint PhD student.

Conflict of interest

The authors declare no conflict of interest.

Keywords: CO_2 adsorption · machine learning · porous carbon · textural properties

How to cite: *Angew. Chem. Int. Ed.* **2019**, *58*, 259 – 263
Angew. Chem. **2019**, *131*, 265 – 269

[1] a) Y. S. Bae, R. Q. Snurr, *Angew. Chem. Int. Ed.* **2011**, *50*, 11586 – 11596; *Angew. Chem.* **2011**, *123*, 11790 – 11801; b) G. P. Hao, W. C. Li, D. Qian, A. H. Lu, *Adv. Mater.* **2010**, *22*, 853 – 857.

[2] a) Y. Li, B. Zou, C. Hu, M. Cao, *Carbon* **2016**, *99*, 79 – 89; b) A. S. Jalilov, G. Ruan, C. C. Hwang, D. E. Schipper, J. J. Tour, Y. Li, H. Fei, E. L. Samuel, J. M. Tour, *ACS Appl. Mater. Interfaces* **2015**, *7*, 1376 – 1382; c) Y. Zeng, R. Zou, Y. Zhao, *Adv. Mater.* **2016**, *28*, 2855 – 2873; d) F. Liu, K. Huang, Q. Wu, S. Dai, *Adv. Mater. Adv. Mater* **2017**, *29*, 1700445; e) D. M. D'Alessandro, B. Smit, J. R. Long, *Angew. Chem. Int. Ed.* **2010**, *49*, 6058 – 6082; *Angew. Chem.* **2010**, *122*, 6194 – 6219.

[3] a) G. Durá, V. L. Budarin, J. A. Castro-Osma, P. S. Shuttleworth, S. C. Quek, J. H. Clark, M. North, *Angew. Chem. Int. Ed.* **2016**, *55*, 9173 – 9177; *Angew. Chem.* **2016**, *128*, 9319 – 9323; b) S. Wang, S. Yan, X. Ma, J. Gong, *Energy Environ. Sci.* **2011**, *4*, 3805 – 3819.

[4] a) R. Banerjee, A. Phan, B. Wang, C. Knobler, H. Furukawa, M. O'keeffe, O. M. Yaghi, *Science* **2008**, *319*, 939 – 943; b) C. Lu, H. Bai, B. Wu, F. Su, J. F. Hwang, *Energy Fuels* **2008**, *22*, 3050 – 3056; c) R. Serna-Guerrero, Y. Belmabkhout, A. Sayari, *Chem. Eng. J.* **2010**, *158*, 513 – 519; d) R. Dawson, E. Stöckel, J. R. Holst, D. J. Adams, A. I. Cooper, *Energy Environ. Sci.* **2011**, *4*, 4239 – 4245; e) P. Li, Y. He, Y. Zhao, L. Weng, H. Wang, R. Krishna, H. Wu, W. Zhou, M. O'Keeffe, Y. Han, *Angew. Chem. Int. Ed.* **2015**, *54*, 574 – 577; *Angew. Chem.* **2015**, *127*, 584 – 587; f) J. Lan, D. Cao, W. Wang, B. Smit, *Acs Nano* **2010**, *4*, 4225 – 4237; g) M. Sevilla, P. Valle-Vigón, A. B. Fuertes, *Adv. Funct. Mater.* **2011**, *21*, 2781 – 2787; h) M. Plaza, C. Pevida, A. Arenillas, F. Rubiera, J. Pis, *Fuel* **2007**, *86*, 2204 – 2212.

[5] a) J. Lee, J. Kim, T. Hyeon, *Adv. Mater.* **2006**, *18*, 2073 – 2094; b) M. M. Titirici, R. J. White, N. Brun, V. L. Budarin, D. S. Su, F. del Monte, J. H. Clark, M. J. MacLachlan, *Chem. Soc. Rev.* **2015**, *44*, 250 – 290; c) H. Wei, S. Deng, B. Hu, Z. Chen, B. Wang, J. Huang, G. Yu, *ChemSusChem* **2012**, *5*, 2354 – 2360; d) D. K. Singh, K. S. Krishna, S. Harish, S. Sampath, M. Eswaramoorthy, *Angew. Chem. Int. Ed.* **2016**, *55*, 2032 – 2036; *Angew. Chem.* **2016**, *128*, 2072 – 2076.

[6] a) R. Wang, P. Wang, X. Yan, J. Lang, C. Peng, Q. Xue, *ACS Appl. Mater. Interfaces* **2012**, *4*, 5800 – 5806; b) A. H. Lu, W. C. Li, E. L. Salabas, B. Spliethoff, F. Schüth, *Chem. Mater.* **2006**, *18*, 2086 – 2094; c) J. R. Maluta, S. A. Machado, U. Chaudhary, J. S. Manzano, L. T. Kubota, I. I. Slowing, *Sens. Actuators A* **2018**, *257*, 347 – 353.

[7] a) W. Shen, S. Zhang, Y. He, J. Li, W. Fan, *J. Mater. Chem.* **2011**, *21*, 14036 – 14040; b) Y. Xia, R. Mokaya, G. S. Walker, Y. Zhu, *Adv. Energy Mater.* **2011**, *1*, 678 – 683; c) M. E. Casco, M. Martínez-Escandell, J. Silvestre-Albero, F. Rodríguez-Reinoso, *Carbon* **2014**, *67*, 230 – 235.

[8] X. Hu, M. Radosz, K. A. Cychosz, M. Thommes, *Environ. Sci. Technol.* **2011**, *45*, 7068 – 7074.

[9] J. He, J. W. F. To, P. C. Psarras, H. Yan, T. Atkinson, R. T. Holmes, D. Nordlund, Z. Bao, J. Wilcox, *Adv. Energy Mater.* **2016**, *6*, 1502491.

[10] S. K. Sinha, M. C. Wang, *Geotech. Geol. Eng.* **2007**, *26*, 47 – 64.

[11] Y. Deng, M. Zhu, D. Xiang, X. Cheng, *Fuel* **2002**, *81*, 1963 – 1970.

[12] a) J. Behler, *Angew. Chem. Int. Ed.* **2017**, *56*, 12828 – 12840; *Angew. Chem.* **2017**, *129*, 13006 – 13020; b) S. Shakeri, A. Ghassemi, M. Hassani, A, Hajian, *Int. J. Adv. Manuf. Tech.* **2008**, *82*, 549 – 557; c) G. Chen, K. Fu, Z. Liang, T. Sema, C. Li, P. Tontiwachwuthikul, R. Idem, *Fuel* **2014**, *126*, 202 – 212; d) Y. Deng, M. Zhu, D. Xiang, X. Cheng, *Fuel* **2002**, *81*, 1963 – 1970.

[13] K. Ryan, J. Lengyel, M. Shatruk, *J. Am. Chem. Soc.* **2018**, *140*, 10158 – 10168.

[14] a) M. H. Segler, T. Kogej, C. Tyrchan, M. P. Waller, *ACS Cent. Sci.* **2018**, *4*, 120 – 131; b) C. W. Coley, R. Barzilay, T. S. Jaakkola, W. H. Green, K. F. Jensen, *ACS Cent. Sci.* **2017**, *3*, 434 – 443; c) A. Mansouri Tehrani, A. O. Oliynyk, M. Parry, Z. Rizvi, S. Couper, F. Lin, L. Miyagi, T. D. Sparks, J. Brgoch, *J. Am. Chem. Soc.* **2018**, *140*, 9844 – 9853.

[15] C. Liang, S. Dai, *J. Am. Chem. Soc.* **2006**, *128*, 5316 – 5317.

Manuscript received: October 27, 2018
Version of record online: December 4, 2018

